

# Experiments investigating Concrete Floor Punching using Specific Reinforcement

A.A. van den Bos<sup>1</sup>, H. Hofmeyer<sup>1,2</sup>

<sup>1</sup> ABT consulting engineers, Civil Engineering Group, Arnhem, The Netherlands,

<sup>2</sup> Technische Universiteit Eindhoven, Structural Design Group, The Netherlands

**To reduce the surface crack width and to optimize the ultimate punching load of warehouse concrete floors, fibre reinforcement and special reinforcement mats above piles are used. Due to the special reinforcement mats, current design rules cannot be used to correctly predict the surface crack width and the ultimate punching load. Therefore, full-scale experiments have been carried out for six different reinforcement types. A fibre-reinforced floor with circular pile mat is the best solution, both for reducing the surface crack width and for optimizing the ultimate punching load.**

*Keywords: Warehouse concrete floors, surface crack width, specific reinforcement, fibre reinforcement, ultimate punching load, experiments.*

## 1 Introduction

The utilization of warehouse floors involves the use of large amounts of material and labour and thus a lot of effort is spent on optimizing the floor design. Because the floor surface is visible and many warehouse floors have to be liquid retaining, owners complain about small cracks, even if they are completely acceptable to the structural engineer. Thus the surface crack width needs to be minimized. Secondly, to design a floor economically, one of the necessarily aspects is a precise prediction of the ultimate punching load. Current design codes are not suitable for finding the surface crack width and ultimate punching load for specific reinforcement types (for instance steel fibre reinforcement). A description and evaluation of the current European and American design codes is given by Albrecht (2002).

On the subject of concrete floor punching, experiments were carried out using normal strength concrete (Richart 1948, Moe 1961, Kinnunen 1960, Andersson 1963, Regan 1984). More recently, punching was studied experimentally using high strength concrete without shear reinforcement (Hallgren 1993, Tomaszewicz 1993, Ramdane 1996). Tests including shear reinforcement were also performed (Oliveira 1999, Lee 1999, Beutel 1998). Furthermore, on high strength lightweight concrete, Osman, Marzouk and Helmy (2000) investigated punching behaviour. All experiments mentioned were merely focused on the ultimate punching load rather than on the surface crack width. However, some research was carried out to compare the ultimate

punching load for plates with fibre reinforcement and traditional bar reinforcement, without addressing the surface crack width (Ding 1999, Alexander 1992, McHarg 2000). New analytical models for determination of the ultimate punching load have been developed (Menétrey 2002, Yankelevsky 1999, Salim 2002). These models predict the ultimate punching load only and do not estimate surface crack behaviour.

To increase the knowledge on surface crack and punching behaviour for specific floor designs (not covered by literature) and possible designs in the future, a research project was started. Eight full-scale experiments were carried out at Technische Universiteit Eindhoven for several floor designs. Hereafter, a finite element model was developed that was verified by the experiments. The finite element model now proves to be a valuable tool in practice, predicting both the crack width and ultimate punching load (Hofmeyer 2005). In this article, the eight full-scale experiments are presented.

## 2 Test specimen

### 2.1 Dimensions

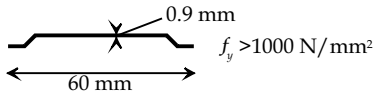
All punching test specimens have dimensions of  $3000 \times 3100 \text{ mm}^2$ , with a thickness of 160 mm.

### 2.2 Material constituents

The punching test specimens are made with fibre reinforced concrete (FRC, specimen 1 to 3) and normal concrete (NC, specimen 4 to 8). For both cases, special (low shrinkage, 160 mm slump) concrete is used with the following constituents: water content  $165 \text{ kg/m}^3$ , cement content  $330 \text{ kg/m}^3$  of which 75% Portland blast furnace cement (ENV 197-1:1992 class III/B) and 25% rapid-hardening Portland cement (type III), coarse aggregate: 75% parts smaller than 32 mm, 25% parts smaller than 16 mm. The fibre reinforced concrete is reinforced with  $35 \text{ kg/m}^3$  Bekaert Dramix RC 65/60 BN, figure 1.

### 2.3 Material properties

To investigate the material properties, material tests were carried out. The cylinder compressive strength after 28 days is  $32.8 \text{ N/mm}^2$  for normal concrete and  $32.0 \text{ N/mm}^2$  for fibre reinforced concrete. Typical results for three-point bending tests after 28 days are shown in figure 2; the beam cross-section equals  $150 \times 150 \text{ mm}^2$ , the span length equals 500 mm. The ultimate load is about equal for the normal and fibre reinforced concrete. For the fibre reinforced concrete, the ratio between ultimate stress and the average tensile stress between 0 and 1.5 mm deflection equals 0.58 (the so-called R1.5 value (CUR 1994), see section 5). Split-tensile strength tests after 28 days yield an average value for FRC equal to  $5.3 \text{ N/mm}^2$  and NC has a splitting tensile strength of  $5.1 \text{ N/mm}^2$ .



Bekaert Dramix RC 65/60 BN

Figure 1: Fibre dimensions.

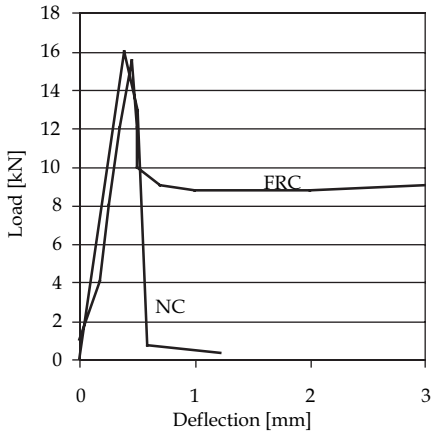


Figure 2: Load vs. deflection for normal (NC) and fibre reinforced concrete (FRC), Three point bending tests ( $150 \times 150 \times 500 \text{ mm}^3$ )

Table 1: Ultimate (punching) load for test specimens.

	Concrete	Reinforcement lay-out	Ultimate load [kN]	Comparison to specimen 4 [%]
1	FRC		361	104
2	FRC	B	458	131
3	FRC	C	440	126
4	NC		349	100
5	NC	B	353	101
6	NC	C	351	100
7	NC	A+B	422	121

- A. Upper mat consists of bars (diameter 8 mm) in each direction, cross-sectional bar distance 100 mm. Positioned over the whole test specimen.
- B. Pile mat consists of 10 bars (diameter 8 mm, length 1000 mm) in each direction, cross-sectional bar distance 100 mm. Upper surface of the mat distance 30 mm. Only positioned above the pile.
- C. Circular pile mat consists of one bar (diameter 8 mm, length 17000 mm) circular bent using an increasing radius of 75 mm for each revolution. On this mat, 7 v-shaped bars (diameter 8 mm,

length 1000 mm) are welded.

- D. Bent-up bars are two trapezoidal 45 degrees bent bars (diameter 8 mm) in each direction, cross-sectional bar distance 200 mm.

### 2.4 Reinforcement

Reinforcement at the top side with 30 mm cover consists of (A) a normal mat, (B) a pile mat, (C) a circular pile mat, (D) bent-up bars, or a combination of A to D, see table 1 and figure 3.

### 2.5 Fabrication

The test specimens for the full-scale experiments were poured at a local contractor (Van Berlo 2003). A list of the test specimens is shown in table 1.

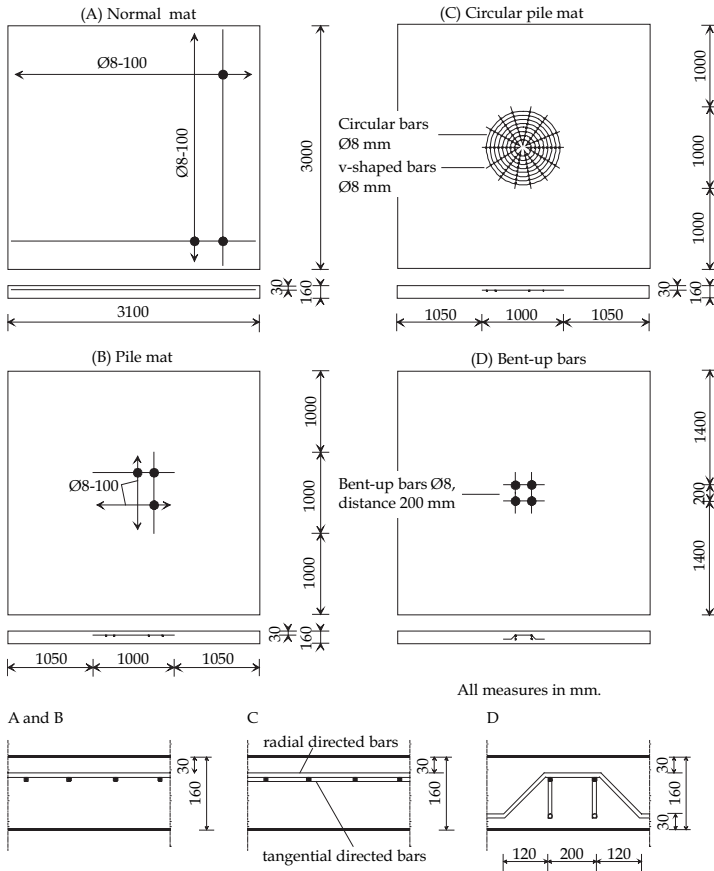


Figure 3: Test specimen dimensions and reinforcement types A to D.

### 3 Test setup

To optimize warehouse floor designs, it should be noted that normal inner floor fields are quantitatively far more present than the boundary floor fields. Furthermore, it was tried to keep the test setup size as small as possible. With regards to these concerns, it was chosen to test a part of the floor above the pile, with a length and width equal to the field width and length, see figure 4.

The equally distributed load in practice is replaced by four fixed supports as shown in figures 5 and 6. A hydraulic jack with a steel loading plate replaces the pile foundation in practice. Thus the pile loads the plate, instead of the distributed load in practice. For a test setup for punching tests Sherif (1996) showed the importance of restraining displacements and rotations at the plate edges. As such, the boundary conditions along the plate edges (in practice an elastic support of the surrounding floor) are replaced by a steel boundary frame that is able to support the plate edges in horizontal and rotational directions. Measurements of the frame deformation show that the frame provides a completely stiff support for the concrete plate.

The four support plates (figure 5) are each fixed to a load cell, recording the total reaction force and the distribution of the reaction forces. An hydraulic jack loads the plate at the bottom side and its hydraulic pressure is used to check the load cell recordings. At the plate top surface, above the hydraulic jack, four Linear Voltage Displacement Transducers (LVDT) measure deformations (elastic strains and crack opening widths) over 300 mm length, figure 7. Along the lines between the four support plates, another four LVDT's measure the crack opening width, see figure 7. Strain gauges (measurement length 12 mm) are positioned at the bottom surface, near the hydraulic jack, and at the top surface, near the corner. Outward displacements of the steel boundary frame are measured at six locations. At two locations, the steel boundary frame rotation is measured. These measurements are used to check the frame effectiveness. During the test, top surface cracks were marked and measured. The last mentioned measurements (not presented) confirm the LVDT measured values.

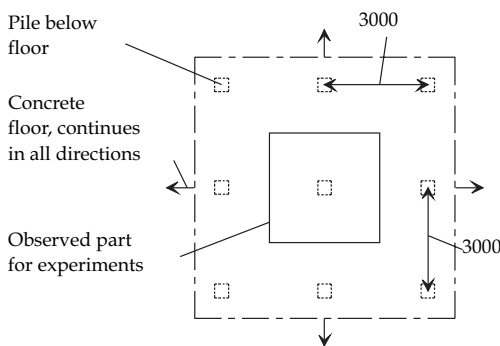


Figure 4: Test specimen represents a part of the warehouse floor, measures in mm.

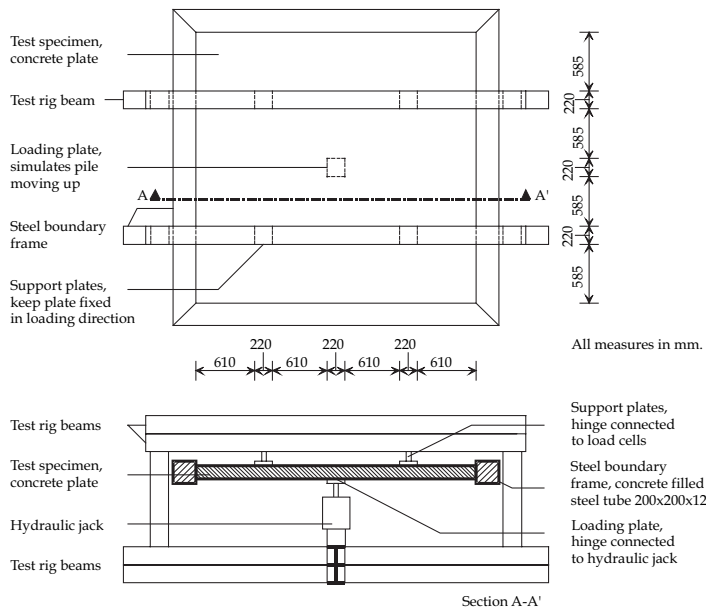


Figure 5: Test rig with test specimen.

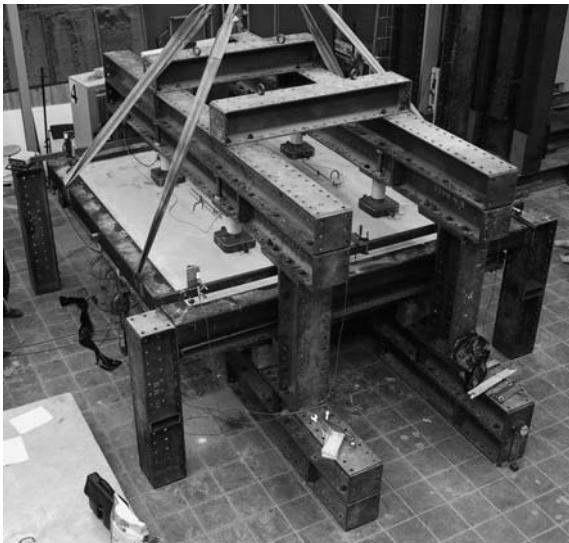


Figure 6: Photo of test rig

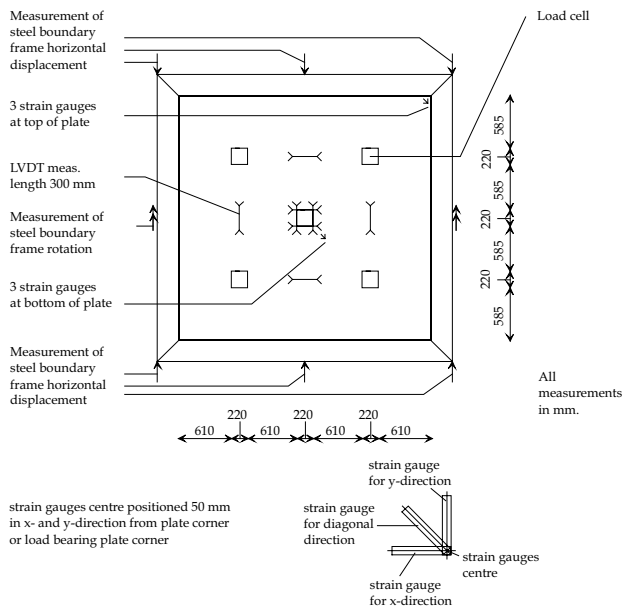


Figure 7: Measurements, top view.

## 4 Experimental results

The punching test specimens are loaded via displacement control by 0.08 mm per second. Results can be grouped in (1) ultimate load and failure, (2) stiffness and crack pattern, (3) LVDT measurements, and (4) strain gauge measurements.

### 4.1 Ultimate load and failure

Table 1 presents the ultimate load found for each test. Figure 8 shows the load-displacement curves for each test. The ultimate load was derived by the sum of the four load cell registrations and was verified by comparing this data with the hydraulic oil pressure of the loading jack. For all tests, the hydraulic jack load is equally distributed over the four load cells. The specimens are thus symmetrically loaded. Fibre reinforced concrete (test 1) results in a 12 kN higher ultimate punching load than non-reinforced concrete (test 4). A pile mat (B), test 5, results in a 4 kN increase of the ultimate punching load compared to the situation without pile mat (test 4). If fibre reinforcement and a pile mat (B) are used together (test 2) the ultimate load increases 109 kN. This indicates that fibre reinforcement and a pile mat (B) improve each others action. It is interesting to note that fibre and a pile mat (B), test 2, perform even better than a pile mat (B) and a normal mat (A) (test 7, for which much more material and labour is needed). Failure is sudden for all tests. The crack pattern functions as a starting grid for the punching cone, figure 9. The cone suddenly breaks out from the floor.

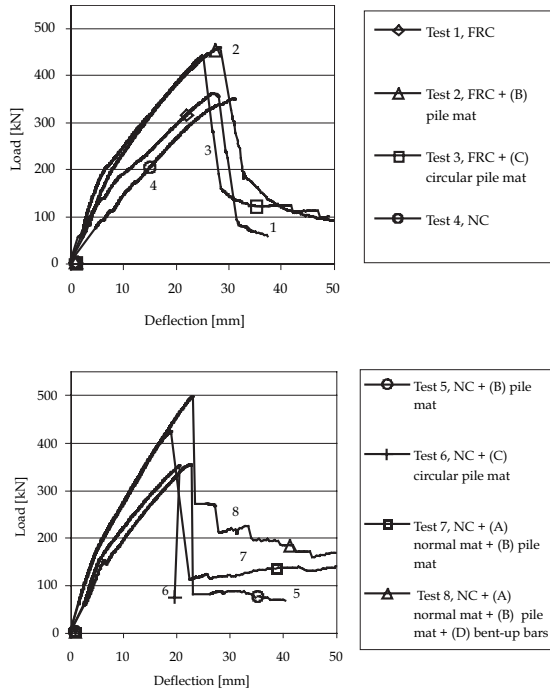


Figure 8: Load-deflection diagrams for all tests.

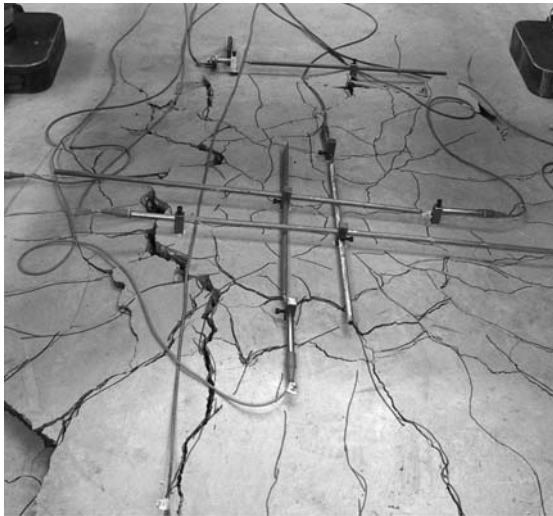


Figure 9: The crack pattern functions as a starting grid for the punching cone, test 8.



#### 4.2 Stiffness and crack pattern

For warehouse floors, flexural stiffness is important for floor surface flatness during serviceability loads. Table 2 shows the stiffness (pile reaction force divided by the plate deflection above the pile) for a serviceability load of 10.75 kN/m<sup>2</sup>. Furthermore, the table shows the amount of surface cracks at ultimate load. For all tests, radial directed cracks are more or less equally spaced and thus the distance between cracks depends on the distance to the plate centre, see figure 9.

Table 2: Stiffness and crack pattern.

Test	Concrete	Reinforcement	Number of radial cracks	Stiffness [N/mm]
1	FRC		9	10092
2	FRC	(B) Pile mat	20	11957
3	FRC	(C) Circular pile mat	27	15278
4	NC		6	9649
5	NC	(B) Pile mat	9	13415
6	NC	(C) Circular pile mat	23	13415
7	NC	(A) Normal mat (B) Pile mat	24	17460
8	NC	(A) Normal mat (B) Pile mat (D) Bent-up bars	24	19097

In general, fibre reinforcement does not increase the floor stiffness for serviceability loads. Traditional reinforcement increases floor stiffness, especially the combination of a normal mat (A) with bent-up bars (D). The number of cracks is related to the crack width: for the same plate deflection, more cracks relate to smaller crack widths. Application of fibre reinforcement does only slightly increase the number of cracks (compare tests 1 and 4). The same is valid for the application of a pile mat (B), as seen in tests 4 and 5. However, the combination of fibre reinforcement and a pile mat (B) leads to a substantial increase of the number of cracks. If no fibre reinforced concrete is used, a circular pile mat (C), test 6, performs slightly better compared to the combination of fibre reinforcement and pile mat (B), test 2. The application of a normal mat (A) and bent-up bars (D) in test 8 does not help to increase the number of cracks compared to test 6 and 7.

### 4.3 LVDT measurements

For every test the number of cracks within the measuring length of a specific LVDT was monitored. Taking test 1, for example, the experiment shows that each LVDT measures over one or two cracks. LVDT measurements range from 1.5 to 4 mm, depending on the location. This results in a crack opening width between  $(1.5/2=) 0.75$  and  $(4/1=) 4$  mm. These results are shown in figure 10 and 11 for all tests. The figures show that the plate without reinforcement (test 4) and the plate with only fibre reinforcement (test 1) show the largest crack widths. Note that fibre reinforcement alone does not significantly reduce crack width. If these two plates (non-reinforced and fibre reinforced only) are improved by the use of a pile mat (normal or circular: tests 2, 3, 5, and 6), crack widths are strongly reduced, not only at the centre, but also along the lines between the supports, figure 11. Finally, for reducing the crack width above the pile, the application of an upper mat (test 7) or punching reinforcement (bent-up bars, test 8) is not useful.

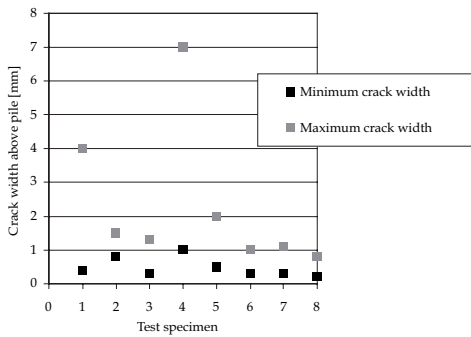


Figure 10: LVDT recorded minimum and maximum crack width values above the pile (radial and/or tangential cracks).

### 4.4 Strain gauge measurements

See figure 7 for strain gauge locations. The strains measured are translated into indicative stresses by multiplication with the Young's modulus (23000 N/mm<sup>2</sup>). Table 3 presents stresses for a serviceability load equal to 10.75 kN/m<sup>2</sup> and at ultimate load.

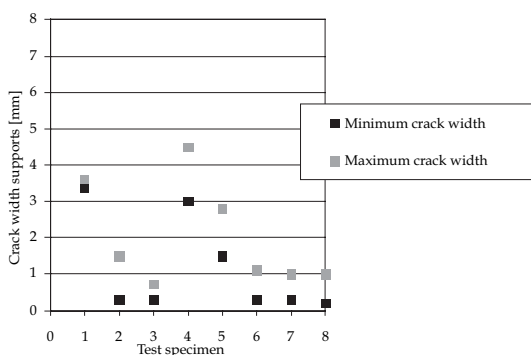


Figure 11: LVDT recorded minimum and maximum crack width values along the lines between the supports (radial cracks).

Table 3: Stresses derived from strain gauge measurements.

Test	Bottom surface, near loading plate		Top surface, at plate corner	
	[N/mm <sup>2</sup> ]		[N/mm <sup>2</sup> ]	
	at 10.75 kN/m <sup>2</sup>	at ultimate load	at 10.75 kN/m <sup>2</sup>	at ultimate load
	<i>x,y, diagonal</i>	<i>x,y, diagonal</i>	<i>x,y, diagonal</i>	<i>x,y, diagonal</i>
1	-3, -5, -2	-13, -22, -7	-, -, -1	-20, -19, 43
2*				
3	-5, -3, -2	-28, -28, -13	0, 0, 0	-8, -8, -27
4	-15, -12, -4	-40, -37, -5	-6, -3, -8	-20, -17, -47
5	-5, -14, -2	-17, -31, -6	0, 0, 0	-1, -13, -34
6	-5, -4, -3	-17, -28, -10	1, 0, 0	11, -7, -28
7	-5, -4, -2	-25, -23, -7	0, 0, 0	0, 6, -16
8	-5, -4, -3	-36, -28, -14	0, 0, 0	-2, -27, -47

\*For test 2, strain gauge locations were different from specified. Therefore, this test cannot be compared with the other tests.

Negative stress values indicate compression, positive values indicate tension. For a load equal to 10.75 kN/m<sup>2</sup>, small stresses occur near the loading plate, which are quantitative comparable for all tests. At the top surface, in the corner of the plate, no stresses occur. At ultimate load, compressive stresses are about equal to the ultimate compressive strength of the concrete. No relation was found between strain gauge measurements (table 3) and number of cracks (table 2) or ultimate punching load (table 1).

## 5 Code equations

Current codes do not include a prediction for the surface crack width (ACI 2002, Eurocode2 2002). However, they provide a prediction of the ultimate punching load for some reinforcement types. In this section, American Standard ACI 318-02 (2002) and Eurocode2 (EC2, 2002) are used, without safety factors, for predicting the ultimate punching load of the section 3 experiments, table 4. American Standard ACI 318-02 predicts the ultimate punching load as follows:

$$V_n = V_c + V_s \quad (1)$$

$$V_c = 2\sqrt{f'_c} b_w d \quad (2)$$

$$V_s = \frac{A_v f_y d}{s} \quad (3)$$

The notation is explained in section "Notation and symbols", after the references. The minimum area of shear reinforcement should be:

$$A_v = 0.75\sqrt{f'_c} \frac{b_w s}{f_y} \quad (4)$$

For EC2, the following formula is used:

$$V_{sd} = \beta d u \tau_{Rd} k (1.2 + 40\rho_1) + \frac{\sum A_{sw} f_{yk} \sin\alpha}{u d} \quad (5)$$

The perimeter of the critical section for punching shear  $u$  is not based on the (equivalent) diameter of the pile head (as for the ACI) but on the diameter of the pile head plus  $1.5d$ . The ACI code predicts the ultimate punching load well. Article 11.5.1. does not permit to use the (A) normal mat, (B) pile mat, and (C) circular pile mat as shear reinforcement. Even the bent-up bars are not allowed as shear reinforcement because the test specimen depth is too low (formula 4). If still a prediction is made, the value permitted is lower than for the non-shear-reinforced sections because for the concrete shear part, a reduced value should be used.

Table 4: Comparison of ultimate punching load from tests and codes.

Test	Type of concrete	Reinforcement	Test [kN]	ACI 318-02 [kN] (ACI/test)	EC2 [kN] (Code/test)	EC2+ FRC adj. [kN] (Code/test)
1	FRC		361			489 (1.35)
2	FRC	B	458			522 (1.14)
3	FRC	C	440			522 (1.19)
4	NC		349	343 (0.98)	411 (1.18)	
5	NC	B	353	343 (0.97)	438 (1.24)	
6	NC	C	351	343 (0.98)	438 (1.25)	
7	NC	A + B	422	343 (0.81)	521 (1.24)	
8	NC	A + B + D	496	291 (0.59)	645 (1.30)	

(A) Normal mat, (B) Pile mat, (C) Circular mat, (D) Bent-up bars

EC2 predicts the failure load too high, but with an almost constant magnification factor. EC2 cannot be used to predict the fibre-reinforced tests. In addition to EC2, it is possible to use an approach that allows an increase of the concrete tensile strength based on the fibre reinforced post-peak behaviour (Brite-Euram 2002). For this approach, the R1.5 value has to be determined which is a measure for the concrete ductility, see section 2.2. This ductility measure can be used to allow for an increase of the tensile strength of the concrete. Based on this approach, for the concrete used here, the Dutch CUR (1994) predicts a R1.5 value equal to 0.54. This allows a 1.34 higher tensile stress (CUR 1994b). Results are shown in the last column of the table and show the same (overestimating) behaviour as for normal concrete.

## 6 Conclusions

Due to fibre reinforcement and special reinforcement mats, current design rules cannot be used to correctly predict the surface crack width and the ultimate punching load for warehouse floors.

Fibre reinforcement only does not increase the ultimate punching load. If a pile mat is used additionally, the ultimate load increases significantly, more than only using the pile mat. Current design codes cannot be used to predict this effect.

LVDT measurements give a good indication of surface crack width behaviour. Fibre reinforcement only does not significantly reduce crack width. If the fibre reinforced plate is improved by the use of a pile mat (normal or circular) crack widths are strongly reduced, much more than with a pile mat only, and even away from the pile (along the lines between the supports). Again, current design codes cannot be used to predict this effect.

Local strain gauge measurements cannot be used to compare or indicate crack width and

punching behaviour for warehouse floors.

EC2 predicts the failure load too high, but with an almost constant magnification factor. The ACI code performs well in this respect but does not permit the use of normal mats (A), pile mats (B), and circular pile mats (C) as shear reinforcement. Even the bent-up bars are not allowed as shear reinforcement because the test specimen depth is too low. However, the experiments show that the bent-up bars significantly increase the ultimate punching load.

## References

- ACI Committee 318 & Portland Cement Association: ACI 318-02, Building Code Requirements for Structural Concrete with Commentary (31802), ACI World Headquarters, 38800 Country Club Drive, Farmington Hills, MI 48331, USA, 2002.
- Albrecht, Uwe: Design of flat slabs for punching – European and North American practices, *Cement and Concrete Composites*, Volume 24, Issue 6, December 2002, Pages 531-538.
- Alexander, S.B.D.; Simmonds, S.H.: Punching Shear Tests of Concrete Slab-Column Joints Containing Fibre Reinforcement, *ACI Structural Journal*, Vol. 89, Issue 4, 1992.
- Andersson JL. Punching of concrete slabs with shear reinforcement. *Transactions* 212, Royal Institute of Technology, Stockholm, 1963.
- Beutel, R.; Hegger, J.: Punching shear resistance of shear reinforced flat slabs, *Arbeitsgemeinschaftindustrieller Forschungsvereinigungen "Otto von Guericke" e.V.*, Research Programm Nr. 10644-N, DBV 185, 1998.
- Brite-Euram BRPR-CT98-0813: Test and Design Methods for Steel Fibre Reinforced Concrete, February 2002.
- CUR 35, Civieltechnisch Centrum Uitvoering Research en Regelgeving: Aanbeveling 35, *Bepaling van de buigtreksterkte, de buigtaaiheid en de equivalente buigtreksterkte van staalvezelbeton*, Stichting CUR, Buchnerweg 3, Postbus 420, 2800 AK Gouda, The Netherlands, 1994.
- CUR 36, Civieltechnisch Centrum Uitvoering Research en Regelgeving: Aanbeveling 36, *Ontwerpen, berekenen en detailleren van bedrijfsvloeren van constructief beton*, Stichting CUR, Buchnerweg 3, Postbus 420, 2800 AK Gouda, The Netherlands, 1994.
- Ding, Yining; Kusterle, Wolfgang: Comparative study of steel fibre-reinforced concrete and steel mesh-reinforced concrete at early ages in panel tests, *Cement and Concrete Research*, Volume 29, Issue 11, November 1999, Pages 1827-1834.
- Eurocode2, CEN (Comité Européen de Normalisation): Eurocode 2, EN1992-1-1 Common rules for buildings and civil engineering structures, CEN, 36 rue de Stassart, B - 1050 Brussels, 2003.
- Hallgren, M.; Kinnunen, S.: Punching shear tests on circular high strength concrete slabs, *Utilization of High Strength Concrete*, Proceedings, Lillehammer, 1993.

- Hofmeyer, H.; Van den Bos, A.A.: Total Strain FE Model for Reinforced Concrete Floors on Piles, submitted to ACI Structural Journal, 2005.
- Kinnunen S, Nylander H.: Punching of concrete slabs without shear reinforcement. Transactions 158, Royal Institute of Technology, Stockholm, 1960.
- Lee, S.C.; Lee, S.B.; Teng, S.; Morley, C.: Punching shear tests on high strength concrete slabs, Fifth International Symposium on the Utilization of High Strength/High Performance Concrete, Proc. Sandefjord, Norway, 1999.
- McHarg, Peter J.; Cook, William D.; Mitchell, Dennis; Yoon, Young-Soo: Benefits of Concentrated Slab Reinforcement and Steel Fibres on Performance of Slab-Column Connections, ACI Structural Journal, Vol. 97, Issue 2, 2000.
- Menétrey, Ph.: Synthesis of punching failure in reinforced concrete, Cement and Concrete Composites, Volume 24, Issue 6, December 2002, Pages 497-507.
- Moe, J.: Shearing strength of reinforced concrete slabs and footings under concentrated loads. Bulletin D47, Portland Cement Association, 1961.
- Oliveira, D.; Melo, G.: Inclined stirrup as shear reinforcement in high performance concrete flat slabs, Fifth International Symposium on the Utilization of High Strength/High Performance Concrete, Proc. Sandefjord, Norway, 1999.
- Osman, M.; Marzouk, H.; Helmy, S: Behaviour of High-Strength Lightweight Concrete Slabs under Ultimate punching loads, ACI Structural Journal, Vol. 97, Issue 3, Pages: 492-498, 2000.
- Ramdane, K.-E.: Punching Shear of High Performance Concrete Slabs, p.1015-1026 in: Utilization of High Strength/High Performance Concrete, Proc. V.3., 1996, Laboratoire Central des Ponts et Chaussées, Paris, 1996.
- Regan, P.E.: The dependence of punching resistance upon the geometry of the failure surface. Mag. Concr. Res. 36 126 (1984), pp. 3–8.
- Richart, F.E.: Reinforced concrete walls and column footings, parts 1 and 2. J. ACI 20 2–3 (1948), pp. 97–127.
- Salim, W.; Sebastian, W.M.: Plasticity Model for Predicting Punching Shear Strengths of Reinforced Concrete Slabs, ACI Structural Journal, Vol. 99, Issue 6, 2002.
- Sherif, A.G.: Behaviour of reinforced concrete flat slabs, Ph.D.-thesis, Dept. of Civil Eng., The Univ. of Calgary, Canada, 1996.
- Tomaszewicz, A.: High-Strength Concrete. SP2-Plates and Shells. Report 2.3 Punching Shear Capacity of Reinforced Concrete Slabs. Report No. STF70 A93082, SINTEF Structures and Concrete, Trondheim, 36 pp., 1993.
- Van Berlo bedrijfsvloeren bv, Binnenveld 11, P.O. Box 183, 5460 AD Veghel, The Netherlands, +31-0413-389090, www.vanberlo.com.
- Yankelevsky, David Z.; Leibowitz, Orit: Punching shear in concrete slabs, International Journal of Mechanical Sciences, Volume 41, Issue 1, January 1999, Pages 1-15.

### Notations and symbols

$V_n$	nominal shear strength, lb.
$V_c$	nominal shear strength provided by concrete, lb.
$V_s$	nominal shear strength provided by shear reinforcement, lb.
$f'_c$	specified compressive strength of concrete, psi.
$b_w$	web width, or diameter of circular section, in.
$d$	distance from extreme compression fiber to centroid of longitudinal tension reinforcement, in.
$A_v$	area of shear reinforcement within a distance $s$ , in. <sup>2</sup>
$s$	spacing of shear or tension reinforcement measured in a direction perpendicular to longitudinal reinforcement, in.
$f_y$	specified yield strength of nonprestressed reinforcement, psi.
$V_{sd}$	Design value of the applied shear force at the ultimate limit state
$\beta$	Coefficient taking account of the effects of eccentricity of load
$d$	Effective depth of a cross-section
$u$	Perimeter of critical section for punching shear
$\tau_{rd}$	Basic shear strength of members without shear reinforcement
$k$	Coefficient which allows for the effects of non-uniform self-equilibrating stresses
$\rho_l$	Equivalent longitudinal reinforcement ratio
$A_{sv}$	Cross-sectional area of shear reinforcement
$f_{yvk}$	Characteristic yield strength of shear reinforcement
$\alpha$	Angle of the shear reinforcement with the longitudinal reinforcement (main steel)